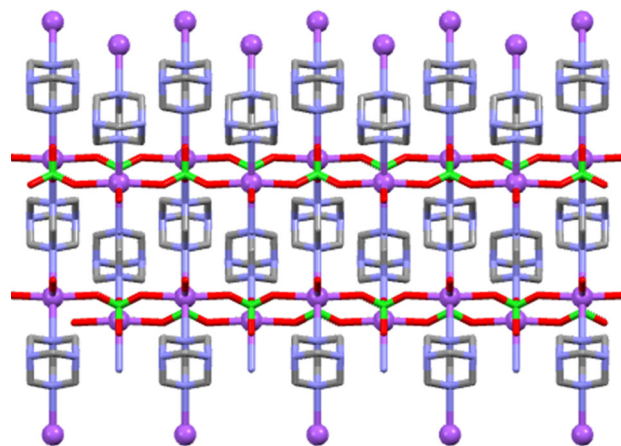CrossMark

ORIGINAL PAPER

On the Coordination Behaviour of the hmta Toward Alkali Metal Cations in Presence of Perchlorate Anions

Rafal Kruszynski[1] · Tomasz Sieranski[1] · Marcin Swiatkowski[1] · Marta Zielak[1] · Jakub Wojciechowski[1] · Magdalena Dzierzawska[1] · Ewelina Czubacka[1]

© The Author(s) 2015. This article is published with open access at Springerlink.com

Abstract The lithium and sodium perchlorate coordination compounds with hexamethylenetetramine of general formulas: $[Li(H_2O)_4]^+ \bullet 2hmta \bullet ClO_4^-$ (**1**) and $[Na(ClO_4)(H_2O)(hmta)]_n$ (**2**) have been synthesized, characterised by elemental and thermal analysis, IR spectroscopy and X-ray crystallography. The compound **2** is a rare three dimensional hybrid compound. The obtained compounds are air stable at room temperature and well soluble in water. As a result of the different electronic properties of the ions, the compounds differ considerably in the molecular structure and consequently in the properties. The studied compounds exhibit opposite placement of both hmta molecules and perchlorate ions: in an outer and inner coordination sphere, respectively, for **1** and **2**. The thermal and spectroscopic properties were correlated with the studied compounds molecular structure.

Graphical Abstract The two novel coordination compounds {namely $[Li(H_2O)_4]^+ \bullet 2hmta \bullet ClO_4^-$ and $[Na(ClO_4)(H_2O)(hmta)]_n$}, of which one is a rare three dimensional hybrid compound, have been synthesized and characterised by: elemental and thermal analysis, IR spectroscopy and X-ray crystallography.

✉ Rafal Kruszynski
rafal.kruszynski@p.lodz.pl

[1] Institute of General and Ecological Chemistry, Lodz University of Technology, Zeromskiego 116, 90-924 Lodz, Poland

Keywords Lithium · Sodium · Perchlorate · Hexamethylenetetramine · Thermal decomposition · IR spectroscopy

Introduction

The study of alkali metal ions bonding in coordination systems has been recently an active area of research [1–6] due to both, the important applications of such compounds (e.g. in medicine [7] and material chemistry [8]) and significance of alkali metal ions in biological systems. Sodium and potassium are present in most, if not in every, known living organisms. They are essential in lots of biological processes such as membrane-transport, metal metabolism (in which lithium ions are often involved as well [9]) as well as they are required for proper functioning of the about one third of natural molecules [10] including enzymes [11], peptides [12] and nucleotides [13]. Hence,

the investigations of alkali metal ions coordination chemistry are currently growing, especially these related to N-donor ligand systems, because such branch of chemistry is considerably unexplored (the 20th century coordination chemistry of the alkali metals were focused mainly on the interactions with O-donor ligands, as extension of the nineteenth century idea, that the alkali metals rather do not form stable compounds with N-donor ligands in presence of the O-donor ligands) [10, 14]. Expanding of this field of research may help to learn of the interaction mechanisms of these metal ions with many bioactive molecules. Additionally the coordination chemistry of the all alkali metals, particularly comparing to transition metals, is still marginally investigated [15–17]. It might seem to be unexpected since many alkali and alkali earth metal–organic compounds are already used in pigments and pharmaceuticals, due to alkali metal advantages (lower toxicity, lower cost, etc.) over the transition and lanthanoid metals [18]. Alkali metal ions are also used to construct dinuclear, multinuclear and polymeric coordination compounds [19–22]. These compounds exhibit interesting and useful properties (e.g. catalytic ones), and the study of interactions existing in their structures helps to understand the origin of these properties. Additionally the studying of the alkali metal ions reactivity toward neutral molecules and determination of the products of the self-organization processes is crucial in supramolecular chemistry and nanotechnology [23–25]. The resolving of the factors governing these self-organization processes is also important in medicine and medicinal chemistry, because such knowledge allows to understand the interaction of the common inorganic ions with the natural and anthropogenic compounds introduced to the human body. All these factors are responsible for the growth of the interest in alkali metal ions coordination chemistry and for such dynamic expansion of the research on influence of subsequent alkali metal ions on formation of the molecular and supramolecular assemblies in a solid-state.

The present study deals with the possibility of differencing the both structures and properties of subsequent alkali metals salts via an N-donor ligand and it is a continuation of investigations of the s block metal ion coordination compounds with the commercially used compound, hexamethylenetetramine (hmta, Scheme 1) [5,
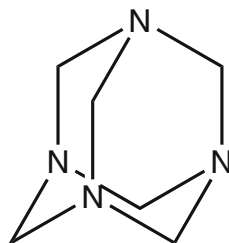
6, 26, 27]. Besides the practical applications (e.g. in phenolic resins production processes as a moulding agent [28, 29], in clinical medicine as an agent for treating urinary tract infections [30]) the hmta is a primary model ligand for tertiary amines and it possesses four exposed nitrogen atoms located at the apexes of a tetrahedron, what is responsible for its versatile applications in construction of multidimensional coordination compounds [31–34]. This strong and bulky shaped organic base, possessing four potential nitrogen donor atoms [35], can act as a crosslinking agent in binuclear and multinuclear coordination compounds [36] and can form up to three dimensional coordination and hybrid architectures. This ligand can also behave as an acceptor of hydrogen bonds making possible its use in construction of versatile supramolecular nets [26, 27, 37], and for these purposes, it is more effective than other N-donor compounds, such as hydrazones [38, 39] and triazolophthalazines [40], semicarbazones [41], thiosemicarbazones [42], hydrazides [43], Schiff bases [44] thiazoles [45] and imines [46]. Moreover, hmta may be used as an outer coordination sphere modulator of an inner coordination sphere [47]. Thus the role of hmta as a building block of coordination compounds cannot be overestimated as it strongly influences the structure and consequently properties of the resulting coordination systems. It must be also noted that the hmta is an inexpensive, commonly available and easily biodegradable reagent, what is an important advantage and this is one of its popularity origins.

The current work explicates the reactivity of the hmta toward the perchlorates of alkali metals, elucidates the influence of the location of the hmta molecules (in an outer and inner coordination sphere) on the rotational-vibrational structure of synthesized compounds (exhibiting in the shifts of IR spectra bands), as well as enlightens the thermal behaviour of the studied compounds.

Experimental

Synthesis

All reactants were the analytical grade and were obtained from POCh S.A. The solutions containing Li^+, Rb^+ and Cs^+ cations (each solution contained only one metal cations) were obtained by dissolution of 0.001 mol of lithium, rubidium and caesium carbonates (0.0740, 0.2303 and 0.3260 g, respectively) in 45 cm³ (Li_2CO_3 and Cs_2CO_3) and in 35 cm³ (Rb_2CO_3) of water, and next the perchloric acid (0.002 mol, 0.11 cm³ of 18.18 mol·dm⁻³ $HClO_4$ standard solution) was added to each carbonate solution. The mixtures were stirred on a magnetic stirrer for about 3 min. The solutions containing Na^+ and K^+

Scheme 1 The hexamethylenetetramine

cations (each solution contained only one metal cations) were obtained by dissolution of 0.001 mol of sodium perchlorate monohydrate and potassium perchlorate (0.1400 and 0.1380 g, respectively) in 3 cm^3 of water. Next, the salt solutions were mixed with hmta aqueous solutions (0.2804 g hmta in 10 cm^3 of water for Li$^+$, Rb$^+$, Cs$^+$, and 0.1402 g hmta in 3 cm^3 of water for Na$^+$, K$^+$) to give 1:1 molar ratio of M:L (metal: ligand). The mixtures were being stirred vigorously on a magnetic stirrer (for about 30 min), then they were placed in a refrigerator and left to crystallize at temperature of 5 °C.

To verify the possibility of formation of compounds with different M:L stoichiometry, all syntheses were repeated with double amount of hmta (0.5608 g dissolved in 20 cm^3 of water, and 0.2804 g dissolved in 10 cm^3 of water, respectively as above). In all cases, after several weeks, the grown crystals were filtered off and dried in air.

The products were initially evaluated via the XRPD and the IR spectroscopy. Only two reactions of the alkali metals (i.e. lithium and sodium) perchlorates with hmta lead to formation of new coordination compounds (both the XRPD patterns and the IR spectra were different from the superposition of the patterns/spectra of the substrates). In case of potassium, rubidium and caesium perchlorates, the substrates crystallised separately, as an inorganic salt (metal perchlorate) and organic ligand (hmta), nevertheless of the metal to ligand molar ratio used in syntheses (the XRPD patterns and the IR spectra were identical with the simple superposition of the patterns/spectra of substrates).

Elemental analyses for studied coordination compounds [Calculated/Found (%)] [Li(H$_2$O)$_4$]$^+$•2hmta•ClO$_4^-$ (**1**): C 31.41/31.50; H 7.03/6.98; O 27.90/27.90; N 24.42/24.57; Li 1.51/1.42; Cl 7.73/7.51; [Na(ClO$_4$)(H$_2$O)(hmta)]$_n$ (**2**): C 25.68/25.74; H 5.03/5.15; O 28.51/28.60; N 19.96/19.87; Na 8.19/8.11; Cl 12.63/12.50.

Crystal Structure Determination

Colourless rectangular prism shape crystals were mounted in turn on a KM-4-CCD automatic diffractometer equipped with the CCD detector, and used for data collection. X-ray intensity data were collected with graphite monochromated CuK_α radiation for lithium compound (to increase the metallic centre scattering of X-ray radiation) MoK_α radiation for sodium compound (to decrease the radiation absorption). The ω scan mode was employed, the 11.1 s exposure time was used for each compound, and all reflections inside Ewald sphere were collected up to $\theta = 68°$ and up to $\theta = 25°$ respectively for **1** and **2.** The unit cell parameters were determined from least-squares refinement of the 611 and 2307 strongest reflections respectively for compounds **1** and **2**. Details concerning crystals data and refinement are given in Table 1.

Examination of reflections on two reference frames monitored after each 20 frames measured did not show decay of the intensity for both compounds. Lorentz, polarization and numerical absorption [48] corrections were applied to the data. The structures were solved by direct methods. All the non-hydrogen atoms were refined anisotropically using full-matrix, least-squares technique on F^2. All hydrogen atoms were found on the difference Fourier syntheses and were refined in riding model. The isotropic displacement factors of the hydrogen atoms were equal to 1.2 and 1.5 times the value of equivalent displacement factor of the patent carbon and oxygen atoms, respectively. The carbon-bonded hydrogen atoms positions were idealised after each cycle of refinement. The three oxygen atoms of ClO$_4^-$ anion of compound **1** are disordered over two domains. Each of these oxygen atom was split into two positions (initially located at the two foci of the distinctly prolating displacement ellipsoid of the atom modelled as non-disordered) and refined with unconstrained positional and displacement parameters. The occupation parameters of these atoms were also refined, but their sum was restrained to 1 for each pairs of atoms and to be equal within one disordered domain. The final refined ratio factor (the second FVAR parameter) was 0.62647. The SHELXS97 [49], SHELXL97 [50] and SHELXTL [51] programs were used for all the calculations. Atomic scattering factors were those incorporated in the computer programs. The selected structural data are given in Tables 2 and 3.

Physical Measurements

IR spectra were recorded on a FTIR Jasco 6200 spectrophotometer in the spectral range 4000–400 cm^{-1} with the samples in the form of KBr pellets. The thermal analyses were carried out in a TG–DTA-SETSYS-16/18 thermoanalyser coupled with ThermoStar (Balzers) mass spectrometer. The samples were heated in corundum crucibles up to 1000 °C at a heating rate of 5 °C/min in air flow. The process temperature ranges were determined by means of thermoanalyser Data Processing Module [52]. The solid products of the thermal decomposition were determined from derivatographic curves. Some transition products of the decomposition were confirmed by X-ray powder diffraction (XRPD) using the Powder Diffraction File [53]. The X-ray powder diffraction (XRPD) patterns were measured in reflection mode on an XPert PRO X-ray powder diffraction system equipped with a Bragg–Brentano PW 3050/65 high resolution goniometer and PW 3011/20 proportional point detector. The Cu $K\alpha_1$ radiation was used. The patterns were measured at 291.0(2) K in the range 2-90° with the narrowest beam attenuator. A diamond powder was used as an internal reference. The samples were sprinkled onto the sample holders using a

Table 1 Crystal data and structure refinement details for studied compounds

Compound	1	2
Empirical formula	$C_{12}H_{32}ClLiN_8O_8$	$C_6H_{14}ClN_4NaO_5$
Formula weight	458.85	280.65
Crystal system, space group	Orthorhombic, $Pna2_1$ (No. 33)	Orthorhombic, $Pnma$ (No. 62)
Temperature (K)	291(2)	291.0(3)
Wavelength (Å)	$\lambda(CuK\alpha)$ 1.54178	$\lambda(MoK\alpha) = 0.71073$
Unit cell dimensions (Å, °)	$a = 26.4543(15)$	$a = 14.6267(10)$
	$b = 9.1315(7)$	$b = 7.0440(4)$
	$c = 8.9091(6)$	$c = 11.1310(6)$
Volume (Å^3)	2152.1(3)	1146.83(12)
Z, Calculated density (Mg m^{-3})	4, 1.416	4, 1.625
Absorption coefficient (mm^{-1})	2.074	0.388
F(000)	976	584
Crystal size (mm)	$0.107 \times 0.099 \times 0.092$	$0.098 \times 0.091 \times 0.073$
θ range for data collection (°)	3.34 to 69.87	2.30 to 25.00
Index ranges	$-31 \leq h \leq 31, -11 \leq k \leq 11, -10 \leq l \leq 10$	$-17 \leq h \leq 17, -8 \leq k \leq 8, -13 \leq l \leq 12$
Reflections collected/unique	23976/3872 [$R_{(int)} = 0.0235$]	11087/1103 [$R_{(int)} = 0.0330$]
Completeness	100 % to $\theta = 68^o$	100 % to $\theta = 25^o$
Min. and max. transmission	0.796 to 0.830	0.957 to 0.969
Refinement method	full-matrix least-squares on F^2	full-matrix least-squares on F^2
Data/restraints/parameters	3872/1/299	1103/0/92
Goodness-of-fit on F^2	1.105	1.098
Final R indices [$I > 2\sigma(I)$]	$R1 = 0.0383$, $wR2 = 0.0962$	$R1 = 0.0268$, $wR2 = 0.0854$
R indices (all data)	$R1 = 0.0384$, $wR2 = 0.0964$	$R1 = 0.0284$, $wR2 = 0.0867$
Largest diff. peak and hole (e Å^{-3})	0.338 and −0.728	0.250 and −0.448

small sieve, to avoid a preferred orientation. The thicknesses of the samples were no more than 0.1 mm. During the measurements each specimen was spun in the specimen plane to improve particle statistics. Elemental analyses were carried out using a Vario EL III CHNOS Elemental Analyzer (C, H, N, O). The alkali metal contents (lithium and sodium) were determined by atomic emission spectroscopy in microwave mineralised samples. Chlorine content was determined by spectrophotometric determination of perchlorate ions with methylene blue [54].

Results and Discussion

The reactions of the alkali metals perchlorates with hmta lead to formation of coordination compounds of lithium and sodium. The potassium, rubidium and caesium perchlorates did not bond to the hmta via coordination bonds or intermolecular interactions (the substrates crystallised separately, as an inorganic salt and organic ligand), nevertheless of the metal to ligand molar ratio used in syntheses (M:L was 1:1 and 1:2). This situation is analogues to the reactions between alkali metals bromides and hmta, in

which only two coordination compounds of whole series were created (i.e. $[Li(H_2O)_4]^+ \bullet hmta \bullet Br^-$ and $[Na(H_2O)_4(hmta)]_2^{2+} \bullet 2H_2O \bullet 2Br^-]$) and other alkali metals bromides crystallised separately from the hmta [5]. The lithium forms the 1:2 (M:L) compound (**1**) and the sodium forms the 1:1 (M:L) compound (**2**), nevertheless of the metal to ligand molar ratio used in syntheses. This is in contrast to the composition of the bromide salts, in which the M:L ratio was always 1:1 [5].

The perspective views of **1** and **2** are shown in Figs. 1 and 2, respectively. All atoms of compound **1** lie in general positions, and the asymmetric unit contains one complex $[Li(H_2O)_4]^+$ cation, two hmta molecules and one, charge balancing, perchlorate anion. This ClO_4^- anion is disordered over two domains in 6.3:3.7 ratio, twisted at about 60° along the local threefold axis going through the Cl11 and O11 atoms. Besides the static disorder, the oxygen atoms of the perchlorate anion show also symptoms of dynamic disorder, what manifests in slightly prolating displacement ellipsoids. The formation of the $[Li(H_2O)_4]^+$ cation is not a common phenomenon. Among the 8299 structurally characterised coordination compounds of lithium only 42 compounds contain such cation [55]. In

Table 2 Selected structural data for studied compounds (Å, °, valence units)

1			**2**		
i—j	d_{ij}	v_{ij}	i—j	d_{ij}	v_{ij}
Li1—O2	1.909(4)	0.302	Na1—O4	2.3370(17)	0.234
Li1—O4	1.932(3)	0.284	Na1—O1	2.3700(11)	0.214
Li1—O1	1.950(3)	0.270	Na1—O3^i	2.441(2)	0.177
Li1—O3	1.971(3)	0.255	Na1—N2^{ii}	2.6611(19)	0.139
			Na1—N1	2.7234(19)	0.117

1		**2**	
i—j—k	α_{ijk}	i—j—k	α_{ijk}
O2—Li1—O4	110.46(18)	O4—Na1—O1^{iii}	90.58(4)
O2—Li1—O1	107.40(17)	O4—Na1—O1	90.58(4)
O4—Li1—O1	117.48(17)	O1—Na1—O1^{iii}	174.02(8)
O2—Li1—O3	111.10(16)	O4—Na1—O3^i	177.72(8)
O4—Li1—O3	106.56(16)	O1^{iii}—Na1—O3^i	89.54(4)
O1—Li1—O3	103.64(17)	O1—Na1—O3^i	89.54(4)
		O4—Na1—N2^{ii}	81.70(6)
		O1^{iii}—Na1—N2^{ii}	87.18(4)
		O1—Na1—N2^{ii}	87.18(4)
		O3^i—Na1—N2^{ii}	100.58(8)
		O4—Na1—N1	82.22(6)
		O1^{iii}—Na1—N1	92.98(4)
		O1—Na1—N1	92.98(4)
		O3^i—Na1—N1	95.49(8)
		N2^{ii}—Na1—N1	163.92(6)

Symmetry codes (i): −x + 1, −y, −z; (ii): x − 0.5, y, −z + 0.5; (iii): x, −y − 0.5, z

Table 3 Hydrogen bonds in studied compounds (Å, °)

	D—H	H···A	D···A	D—H···A
1				
O1—H1O···N4^i	0.95	2.01	2.9558(18)	174.0
O1—H1P···N3^{ii}	0.83	2.22	3.021(2)	163.0
O2—H2O···N12^{iii}	0.99	1.91	2.874(2)	162.1
O2—H2P···N1^{iii}	0.91	1.99	2.880(2)	165.7
O3—H3O···N2	0.96	1.95	2.9051(18)	171.7
O3—H3P···N14^{iv}	0.89	2.10	2.9409(19)	157.3
O4—H4O···N11^v	0.90	2.05	2.940(2)	169.2
O4—H4P···N13^{ii}	0.92	2.02	2.912(2)	163.4
2				
O4—H4O···N3^{vi}	0.85	2.00	2.8504(15)	172.8

Symmetry codes (i): x, y − 1, z; (ii): −x + 1, −y + 1, z + 0.5; (iii): −x + 1, −y + 1, z − 0.5; (iv): x + 0.5, −y + 1.5, z; (v): x + 0.5, −y + 0.5, z; (vi): −x + 1, −y, −z + 1

compound **2** the Na1, Cl1, O2, O3, N1, N2, C1, C4 H4A, and H2B atoms are located at the special position *c* of the *Pnma* space group, with site symmetry m, therefore, the

asymmetric unit contains a half of the [Na(ClO$_4$)(H$_2$O)(hmta)] molecular entity. This reflection plane together with the perpendicular twofold screw axes expand the asymmetric unit to the three dimensional hybrid compound consisting of one dimensional (Na(ClO$_4$))$_n$ double inorganic chains (extending along crystallographic [010] axis) interlinked by the organic ligand. The net nodes located at sodium and chlorine atoms of **2** create the 3,5-c dinodal ((3-c)(5-c) stoichiometry) net, described by {4^2.6^5.8^3}{4^2.6} Schläfli symbol (respectively for {Na}{Cl}atoms) and {4^2.6^5.8(8)}{4^2.6(3)} simplified extended point symbol. This net belongs to the 3,5T1 topological type [56]. The consideration of the hmta cage as an independent trinodal moiety possessing individual tetrahedral topology in the hybrid net leads to {3^3.10.11^2}2{3^3}2{4^2.6.10^4.12^2.16}{4^2.6} Schläfli symbol describing the three dimensional architecture of the 3,3,4,5-c formally 4-nodal net with stoichiometry (3-c)2(3-c)(4-c)2(5-c). The compound **2** is a very rare example of a homonuclear polymeric sodium compound containing the hmta molecule and anion in the inner coordination sphere (only one such compound was synthesised up to date. i.e. the catena-((μ$_3$-hexamethylenetetramine)-tris(μ$_3$-nitrato)-tri-sodium, and, in opposition to **2**, the multidimensionality of the net is achieved by the chelating hexafunctional anions, instead of non-chelating trifunctional anions of **2**) [57]. The lithium cation is four coordinated by four monofunctional oxygen atoms of water molecules, and the sodium cation is six coordinated by two nitrogen atoms of two difunctional-bridging hmta molecules, three oxygen atoms of the three trifunctional-bridging perchlorate anions and one oxygen atom of the terminal water molecule. The coordination polyhedron of the lithium cation can be described as a slightly distorted tetrahedron [58] (the sum of the polyhedron internal interbond angles is 656.64°, what is almost equal to the ideal value of 656.8°) and the sodium cation as a distorted tetragonal bipyramid [59] (Fig. S1, Table 2). In both cases the coordination polyhedrons are the less common ones, i.e. only 33.0 % of lithium coordination compounds possess the coordination environment of an almost ideal tetrahedron, and 23.2 % of sodium cations are surrounded by ligands arranged in the tetragonal bipyramid geometry [55]. The lithium and sodium cations are displaced from the polyhedra centres at 0.038(4) and 0.352(2) Å. The bridging hmta molecules and ClO$_4^−$ ions of **2** are almost asymmetrically bonded to the sodium ions (Table 2). The internal tetragonal planes of compound **2** polyhedron create dihedral angles falling in the range of 88.89(4)°–90.00(0)°.

The bond valences were computed as $v_{ij} = \exp\left[(R_{ij} - d_{ij})/b\right]$ [60, 61], where R_{ij} is the bond-valence parameter (in the formal sense R_{ij} can be considered as a parameter equal to the idealised single-bond length between i and j atoms for given b), d_{ij} is the experimentally
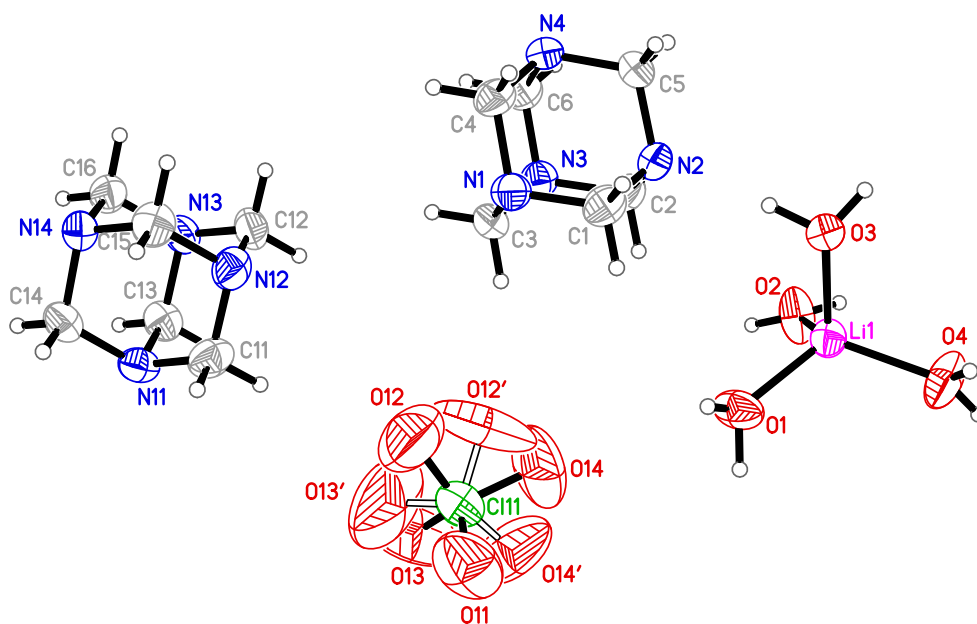
Fig. 1 A view of the compound **1** asymmetric unit, showing the atom-labelling scheme. Displacement ellipsoids are drawn at the 50 % probability level. The hydrogen atoms are drawn as the spheres of arbitrary radii. The disordered part of the perchlorate ion is indicated by *hollow lines*
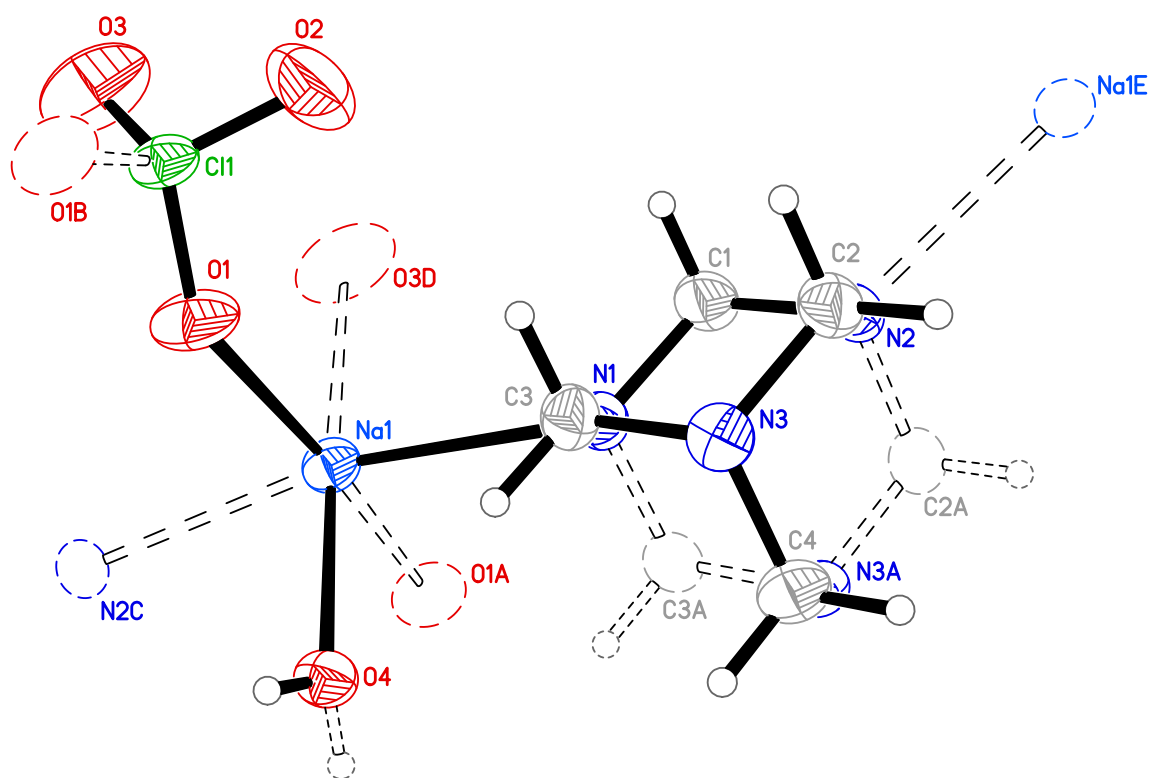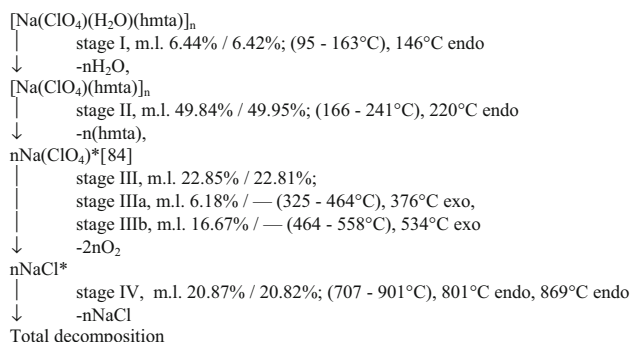

Fig. 2 The molecular depiction of the compound **2** with atom numbering, plotted with 50 % probability of displacement ellipsoids. The hydrogen atoms are drawn as the spheres of arbitrary radii. The symmetry generated atoms (indicated by dashed lines and addition of the letter after the atom number) are obtained by (A): x, −y − 0.5, z; (B) x, −y + 0.5, z; (C) x − 0.5, y, −z + 0.5; (D), −x + 1, −y, −z; (E): x + 0.5, y, −z + 0.5 symmetry transformations

Table 4 Vibrational frequencies [cm^{-1}] and their assignment in studied compounds

Compound **1**	Compound **2**	Lithium perchlorate [85]	Sodium perchlorate monohydrate [85]	Free perchlorate anion [74]	Hmta [86, 87]	Assignment
3441sbr	3486mbr					υ O–H (H$_2$O)
	3370mbr					υ O–H (H$_2$O)
	3177 m					υ O–H (H$_2$O)
	2979vw					υ CH
2963w	2961w				2966	υ CH
2936vw	2937w				2955	υ CH
2892w	2890w				2874	υ CH
	2197w					τ CH$_2$
	2065w					υ CN, CNC deformation
2025vw						υ CN, CNC deformation
	1868vw					υ CN
	1844vw					υ CN
1830vw	1830vw					υ CN
1793vw	1792vw					*ClO$_4^-$
	1770vw					*ClO$_4^-$
	1749vw					*ClO$_4^-$
	1717vw					*ClO$_4^-$
	1669 s					δ O–H (H$_2$O)
1636vs	1636vw					δ O–H (H$_2$O)
1560vw	1570w					*ClO$_4^-$
1542vw	1541w					*ClO$_4^-$
	1522w					*ClO$_4^-$
	1507w					*ClO$_4^-$
	1488w				1489	υ CN, CNC deformation
1465 s	1465 s				1456	σ CH$_2$
	1448vw					σ CH$_2$
	1419vw				1393	CNC deformation
1381 s	1379 s				1370	τ CH$_2$
1352vw	1350vw				1346	ω CH$_2$
	1336w					ω CH$_2$
1238vs	1237vs				1234	υ CN
1147 m	1147 m				1134	υ CN, CNC deformation
1114 m	1113 m	1140	1100	1102		υ_{as} ClO$_4^-$
1087 m	1090 m	1075				υ_{as} ClO$_4^-$
1010vs	1009vs				1007	υ CN
941w	941w				925	υ CN
812 m	817 m				825	υ CN
784vw	783w				779	υ CN
	734w				673	δ N–C–N
688 s	691 m				673	δ N–C–N
	683w				673	δ N–C–N
638w	637w	637				δ ClO$_4^-$
629w	626w			624		δ ClO$_4^-$
510w					512	τ N–C–N

Used symbols: *vw* very weak, *w* weak, *m* medium strength, *s* strong, *vs* very strong, υ stretching, δ bending, ρ rocking, σ scissoring, τ wagging, ω twisting, *br* broad band, *as* asymmetric, * overtone and combination band

$[Li(H_2O)_4]^+ \cdot 2hmta \cdot ClO_4^-$
| stage I, m.l. 7.82% / 7.85%; (25 - 115°C), 106°C endo
↓   -2H₂O
$[Li(H_2O)_2]^+ \cdot 2hmta \cdot ClO_4^-$
| stage II, m.l. 7.83% / 7.85%; (115 - 145ºC), 136°C endo
↓   -2H₂O
$LiClO_4*[83]$, 2hmta*
| stage III, m.l. 74.98% / 75.06%;
| stage IIIa, m.l. 19.81% / — (145 - 214°C), 194°C endo
| stage IIIb, m.l. 22.39% / — (214 - 265°C), 227°C exo
| stage IIIc, m.l. 32.78% / — (265 - 509°C), 361°C exo, 453°C exo
↓   -(hmta, CO₂, CO, NO, NO₂)
LiCl*
| stage IV, m.l. 9.37% / 9.24%; (509 - 793°C), 619°C endo
↓   -LiCl
Total decomposition

$[Na(ClO_4)(H_2O)(hmta)]_n$
| stage I, m.l. 6.44% / 6.42%; (95 - 163°C), 146°C endo
↓   -nH₂O,
$[Na(ClO_4)(hmta)]_n$
| stage II, m.l. 49.84% / 49.95%; (166 - 241°C), 220°C endo
↓   -n(hmta),
$nNa(ClO_4)*[84]$
| stage III, m.l. 22.85% / 22.81%;
| stage IIIa, m.l. 6.18% / — (325 - 464°C), 376°C exo,
| stage IIIb, m.l. 16.67% / — (464 - 558°C), 534°C exo
↓   -2nO₂
nNaCl*
| stage IV, m.l. 20.87% / 20.82%; (707 - 901°C), 801°C endo, 869°C endo
↓   -nNaCl
Total decomposition

Scheme 2 The stages of thermal decomposition of the studied compounds (m.l.—experimental mass loss/theoretical mass loss, *asterisk* product confirmed by XRPD)

determined bond length and b was taken as 0.37 Å [62–65]. The R_{Li-O}, R_{Na-O} and R_{Na-N}, were taken as 1.466, 1.80 and 1.93, respectively [66]. The bond valences approximate the bond strengths (in arbitrary units), as the bond valence theory is, proven to be correct [67, 68], the extension of the Pauling's electrostatic valence rule [69, 70] on the inorganic and coordination compounds. The computed valence of the Li1 and Na1 atom is 1.112 and 1.095 v.u. The small overestimation of the formal oxidation states of lithium and sodium originates from a relative unimpeded coordination sphere of lithium in compound **1** and from constraints imposed by the relatively rigid hybrid net accompanied by presence of unrestrained water molecule in the inner coordination sphere of compound **2**. The coordination bonds of compound **1** have the comparable strength (it differs less than 17 %), however each subsequent bond is slightly weaker than the preceding one (Table 2). The strength of the Na–O bonds is different (the strongest one involve the oxygen atom of the water molecule), but all of them are distinctly stronger than the Na–N bonds. This is in agreement with the hard-soft acid & base coordination chemistry concept, according to which the sodium ion prefers formation of the Na–O bonds over the Na-N bonds [71]. In the structure of compound **1** the multiple intermolecular O(water)—H···N(hmta) hydrogen bonds exist (Table 3) and they create the three dimensional net. The

unitary graph of compound **1** contains only the finite D patterns [72, 73]. The binary graph set contains infinite chain patterns i.e. two $C_2^2(6)$ patterns (Fig. S2–S3) and ten $C_2^2(8)$ patterns (Fig. S4–S13), and does not contain any ring patterns. The cyclic motifs (e.g. $R_4^4(14)$, $R_4^4(16)$, $R_6^6(22)$ and $R_6^6(24)$ patterns) exist in the third and higher level graph sets (Fig. S14–S17). In compound **2** only one hydrogen bond exists and this intramolecular O–H···N interaction forms $S_2^2(12)$ pattern of the lowest degree (Fig. S18–S19) and S(14), $S_2^2(16)$ patterns of the next degrees (Fig. S20–S21).

IR spectra of the studied compounds contain characteristic bands of hmta molecules. In comparison to the pure ligand, the most of them are distinctly shifted to higher frequencies, especially the strongest ones falling in the ranges: 688–691 cm⁻¹ (CNC bending vibrations), 1237–1238 cm⁻¹ (CNC stretching vibrations) and 1379–1381 cm⁻¹ (CH₂ wagging vibrations) (Table 4). The strong band originating from CH₂ scissoring vibrations in the IR spectra of the studied coordination compounds is also shifted to higher frequencies (at about 10 cm⁻¹) in comparison to pure hmta. These shifts are caused by the increase of the excitation energy of the respective oscillators as a result of engaging of the hmta molecules into O–H···N hydrogen bonds. The bands attributed to ClO_4^- vibrations (bending and stretching) are split into two bands in the IR spectra of the studied coordination compounds, while in the IR spectrum of a free perchlorate ion these bands are observed as single bands (Table 4). In a free perchlorate ion the energy levels of the mentioned oscillators are degenerated [74] what simplifies its spectrum. In the IR spectrum of **2** the ClO_4^- overtone bands are most populated (Table 4) as a result of direct coordination of ClO_4^- to the metal cation and consequently larger differentiation of oscillators energies. In **1** the ClO_4^- ion is located in the outer coordination sphere and is not involved into any classical hydrogen bonds, what makes its environment more symmetrical and consequently decreases the population of overtones. In the spectra of both compounds, the characteristic bands originating from OH bending and stretching vibrations of water molecules are present at about 1650 cm⁻¹ and over 3100 cm⁻¹, respectively (Table 4).

The thermal decomposition of the investigated compounds is a gradual process (Scheme 2, Fig. 3). In case of compound **1** the first two endothermic stages of the decomposition are associated with removal of water molecules. When the temperature exceeds 145 °C, the further decomposition begins. In the third stage the hmta is released in three substages (one endothermic sublimation of the hmta and two distinguishable exothermic combustions of the hmta). The first hmta combustion sub-process (IIIb) is accompanied by rapid decomposition of the perchlorate anion (the evolved oxygen probably speeds up the

Fig. 3 TG, DTG and DTA
curves of **a** compound **1** and
b compound **2**
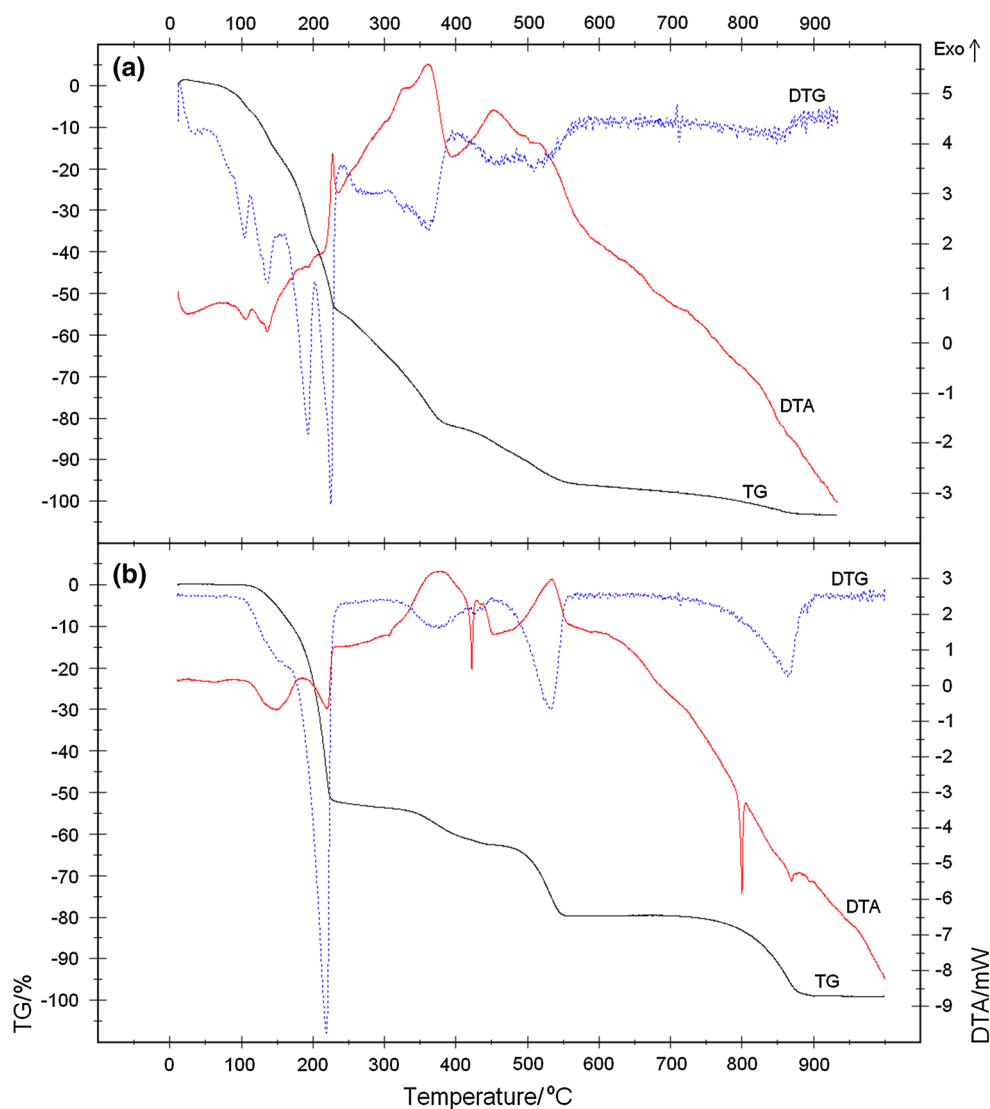
oxidation of the hmta) and formation of lithium chloride as a solid residue (LiClO$_4$ → LiCl + 2O$_2$↑) [75]. The formed salt (LiCl) initially slowly sublimates, then melts (the melting point of LiCl is 617 °C [76]), and finally evaporates in a relativity slow process. The compound **2** is more thermally stable than the compound **1** (Scheme 2) but the initial decomposition stages are analogous. At first, the water molecules are released and next the whole hmta sublimates in an endothermic process. The sodium perchlorate is more thermally stable than lithium perchlorate, thus the oxidation of hmta by the anion decomposition products is not observed. In the third stage the perchlorate ions decompose in two substages (first one slow and in second one rapid), accompanied by maxima on the DTA curve and volatile products mass spectrum curves with m/z = 16 and 32, what confirms the release of the O$^\bullet$ and O$_2$ during this process (NaClO$_4$ → NaCl + 2O$_2$) [77]. The

formed sodium chloride is stable up to 700 °C and with further elevation of the temperature the NaCl starts to sublimate. At about 800 °C the salt melts (the literature melting point of NaCl is 801 °C [78]) and the liquid salt evaporates completely as temperature reaches 901 °C (Scheme 2). The conversion of the perchlorate anions to the chloride anions during thermal decomposition in an oxidative environment is an extremely rare phenomenon, typically, compounds containing this anion explode and/ or are converted directly to the pure oxides [79–82]. The ClO$_4^-$ → Cl$^-$ conversion is possible due to the presence of excess of the reductive amine (hmta: ClO$_4^-$ molar ratio is 2:1) and the basic Li$^+$ cation in case of compound **1**, and the presence of the more basic Na$^+$ cation is the sufficient condition for the conversion of the sodium perchlorate to the sodium chloride in case of compound **2**.

Conclusions

The electronic properties of the cations influence strongly the coordination modes of both hmta molecules and perchlorate anions. The reaction of hmta with lithium and sodium perchlorates leads to the formation of compound containing the ClO_4^- anions and hmta molecules in the outer coordination sphere as well as the compound containing both these anions in the inner coordination sphere. The valence orbital geometry of Li^+ forces the creation of four coordination bonds and the small size of the electron shell disallows the bonding to the Li^+ larger molecular or ionic species, due to steric hindrance. As a result, the charge balancing anion in compound **1** is located in the outer coordination sphere. The presence of 8 relatively strong hydrogen bonds donors in the $[Li(H_2O)_4]^+$ cation forces the building up of the hmta molecules into the crystal net because the sole ClO_4^- anion cannot saturate all of these donors. The compound **2** is a very rare example of a homonuclear polymeric sodium compound containing the hmta molecule and anion in the inner coordination sphere (only one such compound was synthesised up to date. i.e. the catena-((μ_3-hexamethylenetetramine)-tris(μ_3-nitrato)-tri-sodium) [57]. The substantial structural differences affect both the thermal and spectral properties of the investigated compounds. Migration of hmta molecules and perchlorate anions from the outer to the inner coordination sphere and creation of the polymeric compound lead to the increased thermal stability and to more complex rotational-vibrational structure (what causes complication of the IR spectrum). The presented study proves possibility of the usage of simple inorganic anions and organic molecules for construction of the three-dimensional networks possessing high complexity (multinodal nets with complicated stoichiometry) after proper selection of the molecular species for the net self-assembly.

Supplementary Data

Tables of crystal data and structure refinement, anisotropic displacement coefficients, atomic coordinates and equivalent isotropic displacement parameters for non-hydrogen atoms, H-atom coordinates and isotropic displacement parameters, bond lengths and interbond angles have been deposited with the Cambridge Crystallographic Data Centre under no. CCDC1003176 and CCDC1003177, respectively for compounds **1** and **2**.

References

1. Fohlmeister L, Jones C (2014) J Chem Crystallogr 44:301–305
2. Martin-Ramos P, Coutinho JT, Silva MR, Pereira LCJ, Matos Beja AM, Martin-Gil J (2014) J Chem Crystallogr 44:255–260
3. Regulska E, Swislocka R, Samsonowicz M, Lewandowski W (2013) J Mol Struct 1044:173–180
4. Zhou L, Pan S, Su X, Yu H, Yang Z, Zhang F, Zhou Z, Han S (2013) J Mol Struct 1040:80–183
5. Kruszynski R, Sieranski T, Bilinska A, Bernat T, Czubacka E (2012) Struct Chem 23:1643–1656
6. Czubacka E, Kruszynski R, Sieranski T (2012) Struct Chem 23:451–459
7. Rehman S, Ikram M, Khan A, Min S, Azad E, Hofer TS, Mok KH, Baker RJ, Blake AJ, Rehman SU (2013) Chem Cent J 7:110–117
8. Jensen LMR, Abrahams BF, Young CG (2013) J Coord Chem 66:1252–1263
9. Daniele PG, Foti C, Gianguzza A, Prenesti E, Sammartano S (2008) Coord Chem Rev 252:1093–1107
10. Hanusa TP (2005) In: McCleverty JA, Meyer TJ (eds) Comprehensive coordination chemistry II, 2nd edn. Elsevier, Amsterdam
11. Wells CM, Di Cera E (1992) Biochemistry 31:11721–11730
12. Armentrout PB, Gabriel A (2009) Moision. Int J Mass Spectrom 283:56–68
13. Smith RM, Martell AE, Chen Y (1991) Pure Appl Chem 63:1015–1080
14. Das A, Shit S, Kockerling M, Batsanov AS, Mitra S (2013) J Coord Chem 66:2587–2596
15. Pike RD, Dziura TM, deButts JC, Murray CA, Kerr AT, Cahill CL (2013) J Chem Crystallogr 44:42–50
16. Zhao Y, Zhao C, Xu T, Huang Q, Du Z (2014) J Chem Crystallogr 44:480–486
17. De Jesus RN, Ribeiro MA, Inoue MH, Nunes FS, Samulewski RB (2014) J Chem Crystallogr 44:506–511
18. Fromm KM (2008) Coordin Chem Rev 252:856–885
19. Mengle KA, Longenecker EJ, Zeller M, Zaleski CM (2014) J Chem Crystallogr 45:36–43
20. Underwood CC, McMillen CD, Kolis JW (2014) J Chem Crystallogr 44:493–500
21. Read CM, Smith MD (2014) Zur Loye H-C. J Chem Crystallogr 44:604–608
22. Zur Loye KD, Latshaw AM, Smith MD, Chance WM, Zur Loye H-C (2014) J Chem Crystallogr 45:20–25
23. Mafud AC, Sanches EA, Simone CA, Silva ABF, Gambardella MTP (2013) J Mol Struct 1041:1–5
24. Grzelczak M, Vermant J, Furst EM, Liz-Marza LM (2010) ACS Nano 4:3591–3605
25. Sengul A, Kurt O, Buyukgungor O (2011) Struct Chem 22:925–929
26. Sieranski T, Kruszynski R (2013) J Coord Chem 66:42–55
27. Sieranski T, Kruszynski R (2012) J Therm Anal Calorim 109:141–152

28. Pizzi A, Kueny R, Lecoanet F, Massetau B, Carpentier D, Krebs A, Loiseau F, Molina S, Ragoubi M (2009) Ind Crop Prod 30:235–240
29. Choi MH, Chung IJ, Lee JD (2000) Chem Mater 12:2977–2983
30. Greenwood D, Slack RCB (1981) Infection 9:223–227
31. Kruszynski R, Sieranski T, Swiatkowski M, Zielak M, Wojciechowski J, Dzierzawska M, Lewinski B (2014) J Coord Chem 67:1332–1352
32. Hazra S, Naiya S, Sarkar B, Drew MGB, Ghosh A (2013) Polyhedron 65:193–199
33. Kumar D, Kapoor IPS, Singh G, Singh UP, Goel N (2013) J Therm Anal Calorim 114:5–18
34. Kirillov AM (2011) Coordin Chem Rev 255:1603–1622
35. Agwara MO, Ndifon PT, Ndikontar MK (2004) Chem Soc Ethiop 18:143–148
36. Looney MG, Solomon DH (1995) Aust J Chem 48:323–331
37. Vinodu M, Goldberg I (2004) New J Chem 28:1250–1254
38. Trzesowska-Kruszynska A (2013) Cryst Growth Design 13:3892–3900
39. Trzesowska-Kruszynska A (2011) Struct Chem 22:525–535
40. Trzesowska-Kruszynska A (2015) Cryst Eng Comm 17:7702–7716
41. Trzesowska-Kruszynska A (2010) J Mol Struct 917:125–132
42. Trzesowska-Kruszynska A (2014) J Mol Struct 1072:284–290
43. Trzesowska-Kruszynska A (2014) J Coord Chem 67:120–135
44. Trzesowska-Kruszynska A (2012) J Mol Struct 1017:72–78
45. Trzesowska-Kruszynska A (2011) J Coord Chem 64:663–678
46. Trzesowska-Kruszynska A (2010) Struct Chem 21:131–138
47. Trzesowska-Kruszynska A, Kruszynski R, Zalewicz M, Bartczak TJ (2010) J Coord Chem 63:1013–1028
48. X-RED (Version 118) STOE & Cie GmbH, Darmstadt, Germany (1999)
49. Sheldrick GM (1990) Acta Crystallogr A 46:467–473
50. Sheldrick GM (1997) SHELXL97 Program for the solution and refinement of crystal structures, University of Gottingen
51. Sheldrick GM (1990) SHELXTL: Release 41 for siemens crystallographic research systems, University of Gottingen
52. Data Processing Module (Version 14), Copyright 1994–1998 SETARAM, FRANCE
53. Powder Diffraction File International Center of Diffraction Data (2003) 12 Campus Boulevard, Newton Square, PA
54. Nabar GM, Ramachandran CR (1959) Anal Chem 31:263–265
55. Allen FH (2002) Acta Crystallogr B 58:380–388
56. Blatov VA, Shevchenko AP, Serezhkin VN (2000) J Appl Cryst 33:1193–1193
57. Trzesowska A, Kruszynski R (2008) J Coord Chem 61:2167–2177
58. Favas MC, Kepert DL (1980) Prog Inorg Chem 27:325–463
59. Kepert DL (1977) Prog Inorg Chem 23:1–65
60. Zachariasen WH (1978) J Less-Common Met 62:1–7
61. Brown ID (1997) Acta Crystallogr B 53:381–393
62. Brown ID (1992) Acta Crystallogr B 48:553–572
63. Trzesowska A, Kruszynski R, Bartczak TJ (2004) Acta Crystallogr B 60:174–178
64. Trzesowska A, Kruszynski R, Bartczak TJ (2005) Acta Crystallogr B 61:429–434
65. Trzesowska A, Kruszynski R, Bartczak TJ (2006) Acta Crystallogr B 62:745–753
66. Brese NE, O'Keeffe M (1991) Acta Crystallogr B 47:192–197
67. Donnay G, Allmann R (1970) Am Mineral 55:1003–1015
68. Brown ID (2002) The chemical bond in inorganic chemistry: the bond valence model. IUCr Monographs on Crystallography 12, Oxford Science Publications
69. Pauling L (1947) J Am Chem Soc 69:542–553
70. Bragg WL (1930) Zeit Cristallogr 74:237–305
71. Inoue Y (1990) Cation binding by macrocycles: Complexation of cationic species by crown ethers. Marcel Dekker Inc, New York
72. Shimoni L, Glusker JP, Bock CW (1996) J Phys Chem 100:2957–2967
73. Bernstein J, Shimoni L, Davis RE, Chang NL (1995) Angew Chem Int Edit Engl 34:1555–1573
74. Chen Y, Zhang Y-H, Zhao L-J (2004) Phys Chem Chem Phys 6:537–542
75. Cordes HF, Smith SR (1974) J Phys Chem 78:773–776
76. Kamali AR, Fray DJ, Schwandt C (2011) J Therm Anal Calorim 104:619–626
77. Marvin GG, Woolaver LB (1945) Ind Eng Chem 17:474–476
78. Cucos A, Budrugeac P, Mitrea S, Hajdu C (2013) J Therm Anal Calorim 111:467–473
79. Singh G, Baranwal BP, Kapoor IPS, Kumar D, Frohlich R (2007) J Phys Chem A 111:12972–12976
80. Singh CP, Singh A, Daniliuc CG, Kumar B, Singh G (2015) J Therm Anal Calorim 121:633–640
81. Vecchio S, Materazzi S, Wo LW, De Angleis CS (2013) Thermochim Acta 568:31–37
82. Singh G, Kapoor IPS, Kumar D, Singh UP, Goel N (2009) Inorg Chim Acta 362:4091–4098
83. Wickleder MS (2003) Z Anorg Allg Chem 629:1466–1468
84. Zachariasen WH (1930) Z Kristallogr Kris 73:141–146
85. Miller FA, Wilkins CH (1952) Anal Chem 24:1253–1294
86. Bernstein MP, Sandford SA, Allamandola LJ, Chang S (1994) J Phys Chem 98:12206–12210
87. Jensen JO (2002) Spectrochim Acta A 58:1347–1364